Available online at www.sciencedirect.com

ScienceDirect

Procedia Manufacturing 47 (2020) 1036–1042

Procedia MANUFACTURING

www.elsevier.com/locate/procedia

23rd International Conference on Material Forming (ESAFORM 2020)

Influence of Conventional Machining on Chemical Finishing of Ti6Al4V Electron Beam Melting Parts

Laurent Spitaels[a,*], François Ducobu[a], Anthonin Demarbaix[a], Edouard Rivière-Lorphèvre[a], Pierre Dehombreux[a]

[a]*Machine Design and Production Engineering Lab - Faculty of Engineering - University of Mons, Place du parc 20, 7000 Mons, Belgium*

* Corresponding author E-*mail address:* laurent.spitaels@umons.ac.be

Abstract

Additive manufacturing is feeding great hopes for future developments in fields such as aeronautical, biomedical and rapid tooling industrssssies. However, limitations are still restricting its use to make prototypes and hampering mass production. In the case of titanium alloy printing (e.g. Ti6Al4V) with the EBM (Electron Beam Melting) process, the major obstacle to use parts directly after printing is their roughness (Arithmetic Roughness (Ra) ~25 µm). Even if the parts are better regarding residual stresses than parts coming from other 3D printing processes, the high roughness decreases their fatigue resistance. A set of parts were manufactured in Ti6Al4V by EBM process. Their characteristics in terms of dimension (cylindricity and diameter) and surface (Arithmetic Roughness Ra and Total Roughness Rt) were evaluated directly after printing. The average Rt stands at 96 µm e.g. The parts endorsed then a first chemical etching to remove the peaks and valleys on their surface. The average Rt decreased at 90 µm e.g. Afterwards, a robotic machining was performed to remove a layer of 400 µm to reach the core material of the part. The average Rt obtained was 5 µm e.g. Finally, a second chemical etching with the same parameters as the first was done. The average Rt increased finally to 9 µm e.g. The same set of dimensional and surface measurements were made after each step of the experimental setup. The succession of operations and measurements allows to compare the influence of conventional machining on the chemical finishing performed on the parts. Furthermore, the machining emphasizes the apparition of surface defects due to the use of a robot (tessellation). Finally, a Rt degradation and a surface finish change have been recorded after the second chemical etching. Perspectives can be focused on assessing these last observations by repeating the experimental setup with more parts.

Keywords: Electron Beam Melting (EBM); Chemical Etching; Ti6Al4V; Metrology; Roughnes

1. Introduction and context

1.1. Additive Manufacturing

Additive Manufacturing (AM) is gaining more popularity since the last 20 years and feeds wide expectations for Industry 4.0. [1,2]. The main advantage achieved by AM is the production of near net shape parts with complex geometry while using less material than conventional manufacturing processes [3]. This allows to make rapid prototypes, produce small and intermediate series of goods without investing in costly equipment and unlock design limitations. Aeronautical and biomedical industries have strong interest in the available AM technologies and their current capabilities [3]. Nonetheless, limitations such as lack of standards, slowness in production and rough surfaces are still limiting their use in mass industry [2]. Additive manufactured parts also suffer from surface defects [4]. These lasts impact the mechanical properties of the parts and reduce their ability to resist to fatigue. Finishing treatments are then mandatory to improve

10.1016/j.promfg.2020.04.321

these mechanical properties in order to reach the same performance as parts produced by conventional processes.

1.2. Titanium alloys

In the wide range of printable products, titanium alloys are widely used in medical, aeronautical and chemical fields. In this family, Ti6Al4V is, as said by Liu and Shin [5], the most popular with plenty of applications thanks to its properties in terms of strength-to-weight ratio, biocompatibility and corrosion resistance [6]. This alloy is mostly printed with three current processes: DED (Direct Energy Deposition), SLM (Selective Laser Melting) and EBM (Electron Beam Melting) [7].

EBM process is less studied than SLM but feeds great hopes due to the mechanical properties of the parts produced (compressive residual stresses), its capability to produce components with a higher building rate and a lower porosity than SLM [5]. However, this faster printing goes with an increased roughness (Arithmetic Roughness (Ra) ~25 µm) with respect to the other processes. This roughness is a weakness for the parts when they are under stresses and does not allow a direct use for specific mechanical applications (contact e.g.). Indeed, in addition to be ineffective in terms of mechanical resistance, every irregularity of this rough surface can act as a crack initiator [4] and leads to poor fatigue resistance of the parts directly used after printing.

1.3. Chemical etching

Several processes exist to improve the surface finish [2,8]. They can be sorted into mechanical treatments [8]: shot-peening, tribofinishing, vibratory finishing, conventional machining, laser polishing or also non-conventional techniques like shape adaptative grinding [9] and in electrochemical treatments [8]: chemical etching, electrochemical polishing and plasma electrolytic polishing. In this available panel, chemical etching is one of the most promising answer to improve the surface state because it can be applied to any complex geometry (e.g. lattice structures), does not need big investment and does not induce mechanical stresses on the part surface. Moreover, this process allows a complete part treatment [10] and has already shown good results for lattice structures finishing treatments [11,12]. Conventional finishing treatments have also shown their limitations when treating titanium alloys: e.g. build-up on the tool edge during machining and fast wear of wheel during grinding [13].

Different types of acids can be used depending of the finishing operation required. As explained by Wysocki et al. [14] in the case of scaffolds structures (lattice), the more efficient chemical etching to remove unmelted titanium particles is made by using a mix of HF and HNO_3. Indeed, if only HF was used, then hydrogen embrittlement would have been promoted and the chemical bath could have been more difficult to control. Consequently, the chemical etching chosen for the experiments shown in this article is composed of a mix of HF and HNO_3 as also used in the literature [11–13,15,16].

This article compares the achievable roughness of Ti6Al4V EBM parts chemically finished before and after robotic machining. This study allows to compare the material composing the part surface and its core, together with their influence on chemical etching. For this reason, a set of measurements is performed with diameter, cylindricity and roughness measurements (Arithmetic Roughness Ra and Total Roughness Rt) of the treated parts.

2. Parts manufacturing

The geometry of the parts used in this study is given in Fig. 1(b). They were printed by EBM process on an ARCAM A2 machine. The part design is fitted with two different cylinder diameters (diameter a and b) as depicted in Fig. 1 (a). The building direction of the samples was set along their Z axis. Standard ARCAM parameters for 50 µm layers were used. The total height targeted was 27.450 mm and diameters a and b were respectively set at 9.660 mm and 21.070 mm. In total 24 parts were produced in the same batch. The resulting part geometry is shown in Fig. 1 (b) with a standard centimeter rule.

The part material is Ti6Al4V ELI (Extra Low Interstitial) Grade 23. Printing was performed with spherical plasma atomized ARCAM powder of this last material. Granulometry distribution of the powder is between 45 µm and 106 µm. The D50 is centered on 70 µm and no Hipping operation was performed.

6 parts were selected from the batch. They were chosen according to their position on the building plate of the EBM machine. This choice was made in order to have parts with the same thermal history and, consequently, the same metallurgical and mechanical properties. These first 6 parts coming from the 3D printing machine without any further treatment are named “raw parts” in the following sections. Each part has been given a letter from A to F to record the different measurements performed on it.

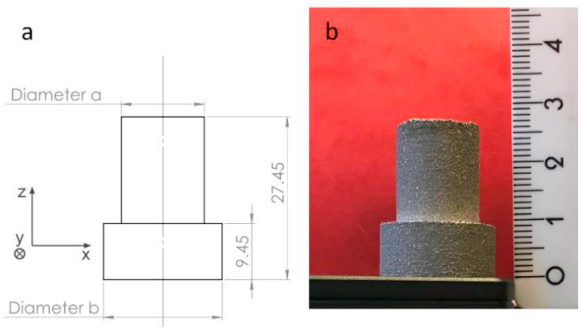

Fig. 1. (a) Sample design and coordinate axis; (b) Resulting part geometry

3. Experimental setup

In order to emphasize the influence of conventional machining on chemical finishing, 4 steps were set up in the experimental study:

- 0 - Preliminary analysis;
- 1 - First chemical etching;

- 2 - Robotic milling;
- 3 - Second chemical etching.

The figures of sections 4, 5 and 6 use the numbers in front of each step.

3.1. Preliminary analysis

The first step of experimental setup was dedicated to performing dimensional and surface roughness measurements on the raw parts. Indicators such as Arithmetic Roughness (Ra) and Total Roughness (Rt) were measured to characterize the surface quality of the parts. These measurements were performed on a Diavite DH-6 machine. Acquisition of the signal was made by a computer and Ra and Rt calculations were performed under the software Diasoft version 3.1.9. It should be noted that arithmetic and total roughness were measured along a direction parallel to the axis of the part cylinders. In order to have a complete overview of all the cylinder roughness, 5 measurements spaced by 72 ° (rotation with respect to Z axis) were performed on each part.

Cylindricity and diameter measurements were performed using a Wenzel LH54 coordinate measuring machine (CMM) with a Renishaw head PH10M and a Renishaw TP20 spherical probe of 2.5 mm diameter. It should be noted that the measurements were made without a regulated temperature in the room. Temperature varied approximately between 18°C and 21°C and this variation was considered within the error calculations (contribution of ± 0.55 µm on each result). Almost all measurements described are made on the cylinder of diameter b. The cylinder of diameter a is used to hold the part during measuring or milling operations.

3.2. First chemical etching

The next experimental step is the first chemical etching. This was carried out in order to remove a thickness equivalent to the total roughness measured during the first step. All bath parameters are not given since it is the know-how of the company having processed the parts. The only available information is the ratio between nitric and hydrofluoric acid. This stands at 20. As shown in section 4.2, the Rt measured varies between 82.04 and 110.20 µm. Consequently, to be sure to take off Rt, a target layer of 150 µm was asked to be removed. The aim of this operation is to discard the peaks and valleys existing on the part surface.

After analysis it was shown that a layer of ~ 250 µm was removed identically on all parts during this first chemical etching. This last measurement shows also that the chemical bath acted equally on all parts treated. The same set of dimensional and surface measurements, as for preliminary analysis, was then performed again to compare the chemically etched parts with the raw parts.

3.3. Robotic milling

The third phase consists in removing a sufficient layer on the part in order to get rid of the remaining roughness coming from the printing process. The layer removed on each part is 400 µm. The machining was performed using a milling robot Staubli TX200 fitted with a Teknomotor ATC71 electro-spindle. The milling tool selected is a SECO JS512050 D2C0Z2 NXT with a diameter of 5 mm and 2 teeth. Standard cutting conditions recommended by SECO for this tool in Ti6Al4V were used but without lubrication:

- Feed per tooth f_z = 0.026 mm/tooth;
- Cutting speed v_c = 95 m/min;
- Feed speed v_f = 314 mm/min;
- Radial depth of cut a_e = 200 µm;
- Axial depth of cut a_p = 500 µm.

2 radial passes of 200 µm were performed with the robot with an axial depth of cut of 500 µm to ensure the best achievable roughness. After robotic milling, the same set of analysis, as for preliminary analysis, was made for dimensional and surface characterization. As it is described in section 6, the robotic milling induced new surface defects (tessellation) due to its reduced capability to achieve geometrical trajectories of small diameter with respect to its working zone.

3.4. Second chemical etching

The last step of analysis is a second chemical etching on the parts. The same bath parameters were used and the ratio between nitric and hydrofluoric acid remains at 20. The layer asked to be removed is the same as for step one in order to be in the same operating conditions. So, the target layer to be removed stands at 150 µm. After analysis it was shown that an average layer of 85 µm was removed identically on all parts. Finally, the Ra, Rt, diameter and cylindricity measurements were performed a last time to allow a comparison of this step with the 3 previous ones.

3.5. Witness samples for visual analysis

A part was chosen after each step, in order to act as a witness of the operations performed. So, after the step zero, part A was kept, and the other ones were chemically etched. After step one, part B and C were kept, and the other ones were robotically milled. Part C was kept because it was the witness used to calibrate the first chemical bath. After step two, part D was kept, and only parts E and F endorsed the last chemical etching. In these last two parts, F was the one chosen to calibrate the last bath. Fig. 2 shows the different witnesses after each step of the experimental setup.

Fig. 2 allows to carry out a visual evaluation of the part cylinder of diameter b after each experimental step. After the first chemical etching, the part surface seems to be more homogeneous in terms of roughness. However, it is still high as it is presented in section 4. Robotic milling allows to obtain a shiny finish while the last chemical etching decreases the shiny finish and leads to a duller surface.

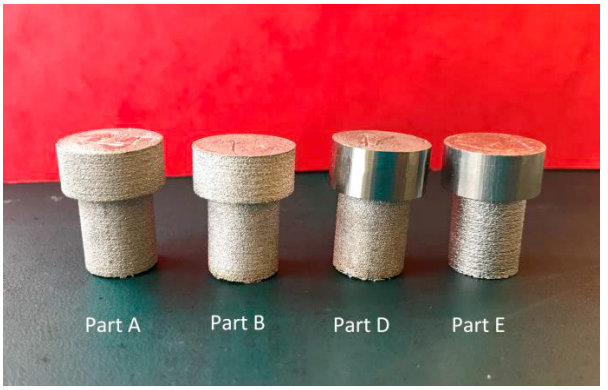

Fig. 2. Witnesses of the experimental steps

4. Arithmetic and total roughness measurements

Each part result presented in the following sections is an average of five measurements. For each set of data, a standard deviation (σ) has been computed. 2σ is used as error bar on the figures in order to have 95% of the results contained in the interval: result ± 2σ. All the measurements were made on the cylinder of diameter b with an evaluation length of 4.8 mm.

The results obtained for Ra and Rt before robotic milling do not fulfill ISO 4288 [17] because, as the roughness is between 13.14 µm and 17.40 µm, the evaluation length to choose would have been of minimum 40 mm. However, the available average length of the cylinder is 9.45 mm and does not allow to analyze roughness profile with the recommended length. Consequently, Ra and Rt measurements can only be used to have a qualitative point of view of the decrease or increase of roughness.

4.1. Arithmetic roughness measurements

Fig. 3 compares the arithmetic roughness (Ra) measurements after each step of the experimental setup. For raw parts coming directly from the 3D printing machine, the Ra starts between 13 and 17 µm. These measured values are better than the ones found in literature [8,16]. As explained by Nutal in [8], this can be due to the too short evaluation length with respect to ISO 4288 recommendations [17].

The first chemical etching decreases roughness only by 2.5%. This observation is confirmed by Dolimont et al. [16]. Part D had also a higher roughness after first etching than before without any visual signs of degradation on the part. However, the surface after chemical etching seems to be still rough visually but better than before as shown by Dolimont [2].

Roughness decreases dramatically after robotic milling and reaches results < 0.5 µm for some parts (reduction of 97%). This last roughness result allows to foresee demanding application of the treated part cylinder according recommendation of Ra < 1.6 µm for contact surface. Same range of results was measured by Bagehorn et al. [10]. This remaining roughness, with respect to the thickness removed, is mainly due to milling parameters and is not coming from initial raw parts roughness.

The last chemical etching does not affect the arithmetic roughness which stands at the same level as after robotic milling.

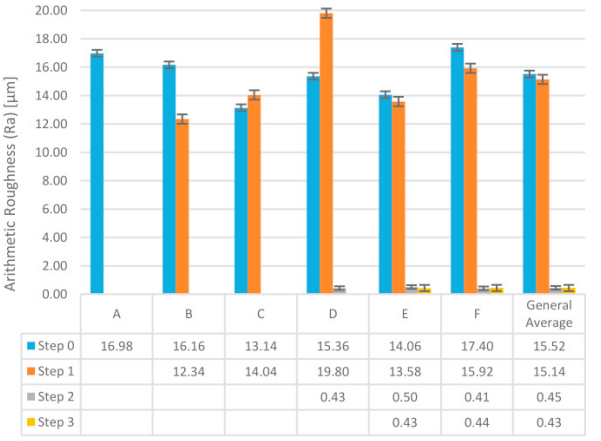

	A	B	C	D	E	F	General Average
Step 0	16.98	16.16	13.14	15.36	14.06	17.40	15.52
Step 1		12.34	14.04	19.80	13.58	15.92	15.14
Step 2				0.43	0.50	0.41	0.45
Step 3					0.43	0.44	0.43

Fig. 3 Arithmetic Roughness [µm]

4.2. Total roughness measurements

The measurements of total roughness for the parts after each step of the experimental setup are given in Fig. 4. The same observations as arithmetic roughness measurements can be made. So, total roughness is decreased by 6.5% after the first chemical etching from an average value of 96.27 µm to 90.04 µm. So, even if a layer of 250 µm is removed, the roughness peaks and valleys are still on the parts and do not allow to destine them directly to a mechanical demanding application such as contact. Even though, the first chemical etching allows to homogenize the total roughness of the parts (except for part D for which total roughness was measured higher after chemical etching than before). This last observation confirms the visual analysis.

The robotic milling decreases the Rt from an average of 90.04 µm to 4.72 µm, so a reduction of 95%. These results demonstrate that the peaks and valleys composing the raw parts roughness have been taken off efficiently by robotic milling. The remaining roughness comes from the robotic milling operation itself.

The measurements made after the last chemical etching show a degradation of Rt (increase of 83% of the value after robotic milling). The part with the highest degradation (part F) is the one which has undergone a longer chemical etching since it was the witness used to calibrate the bath. This can be a consequence of the last chemical etching applied on the material composing the core of the part. It would be interesting to continue with more parts to assess this result. As explained before, these measurements are made on only two parts.

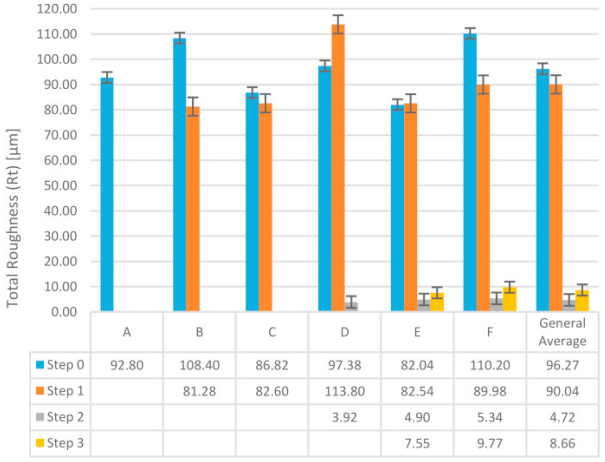

	A	B	C	D	E	F	General Average
Step 0	92.80	108.40	86.82	97.38	82.04	110.20	96.27
Step 1		81.28	82.60	113.80	82.54	89.98	90.04
Step 2				3.92	4.90	5.34	4.72
Step 3					7.55	9.77	8.66

Fig. 4. Total Roughness [µm]

4.3. *Complementary Ra and Rt measurements*

As explained in section 3, all treatments were focused on the cylinder of diameter b. Nevertheless, Ra and Rt measurements were also performed on the cylinder of diameter a after the second chemical etching. Indeessd, this cylinder received two chemical etching treatments without robotic milling in between. So, comparing their respective roughness allows to highlight the contribution of roughness improvement of the second chemical bath as if it was performed without robotic milling. The assumption that chemical etching is acting with the same efficiency on all the sample cylinders and that roughness is homogeneous on all the part after printing are made.

Results are presented in Fig. 5. The ones for Step 0 (Preliminary analysis) and Step 1 (After first chemical batch) were made on cylinder of diameter b while the results showed for Step 3 (After second chemical bath) were obtained by measuring roughness on the cylinder of diameter a. As before, each measurement was repeated five times. All of these were performed at 72° from each other. Error bars are computed by using a 2σ approach.

Conclusion about this figure is that, even after the first bath, it is still possible to improve by approximately 30% the arithmetic and total roughness of the parts. The conclusions are the same as shown in section 4.1 for the improvement between step 0 and 1.

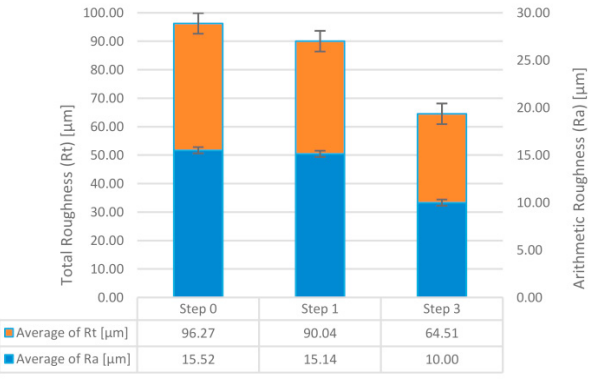

	Step 0	Step 1	Step 3
Average of Rt [µm]	96.27	90.04	64.51
Average of Ra [µm]	15.52	15.14	10.00

Fig. 5. Complementary measurements of Ra [µm] and Rt [µm]

5. Diameter measurements

Fig. 6 shows the diameter measurements after each step of experimental setup. Each measuring point was obtained by probing 8 points spread over two circles at two different heights with respect to the Z axis of the parts. The average diameter of the best cylinder passing by these points was then computed.

As expected, it decreases after each experimental step. After all different phases, an average of 1.453 mm of material was removed on each part cylinder of diameter b. Error bars are computed by using a 2σ approach.

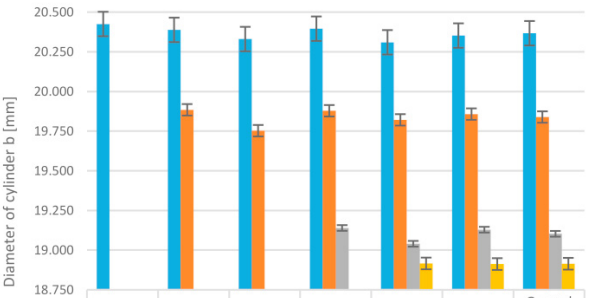

	A	B	C	D	E	F	General average
Step 0	20.425	20.388	20.330	20.395	20.310	20.352	20.367
Step 1		19.884	19.753	19.878	19.821	19.857	19.839
Step 2				19.140	19.040	19.129	19.103
Step 3					18.916	18.912	18.914

Fig. 6 Diameter of cylinder b [mm]

6. Cylindricity measurements

The results of cylindricity measurements are given in Fig. 7. Each measuring point was obtained by probing 8 points spread over two circles at two different heights with respect to the Z axis of the parts. The standard radial deviation from the two probed circles was then computed in order to obtain the cylindricity. The measurement error bars are also computed by taking a 2σ approach.

Measurements on raw parts indicate that, even if parts in the same region of the building plate were chosen, they do not have the same characteristic in terms of cylindricity (σ = 0.027 mm

for an average cylindricity of 0.062 mm). These results are still in the same range after the first chemical etching.

On the other hand, cylindricity is three times worse after robotic milling. This is due to the process chosen of robotic milling and the poor robot capacity to interpolate a circular trajectory of small diameter with respect to the robot size. It can be seen visually on the parts machined that the surface has new defects (tessellation) which appeared after their machining.

The second chemical etching does not allow to improve this defect. Consequently, the results of cylindricity after second chemical etching are still on the same range as before and chemical etching does not affect part cylindricity.

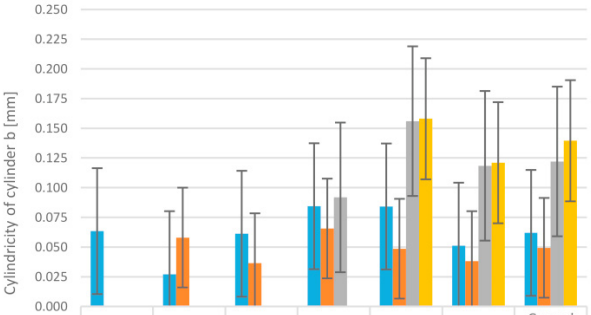

	A	B	C	D	E	F	General average
Step 0	0.063	0.027	0.061	0.084	0.084	0.051	0.062
Step 1		0.058	0.036	0.066	0.049	0.038	0.049
Step 2				0.092	0.156	0.118	0.122
Step 3					0.158	0.121	0.140

Fig. 7 Cylindricity of cylinder b [mm]

7. Conclusion

Parts were obtained by EBM process in Ti6Al4V. These parts have undergone a first chemical etching followed by a robotic milling. The last treatment was a second chemical etching with the same parameters as the first one. Dimensional and surface parameters were measured before the first experimental step and the after each operation.

Arithmetic roughness was not much affected by the first chemical etching (decrease of only 2.5%). The robotic milling allowed to decrease Ra dramatically (by 97%) and to obtain a shiny finish. The last chemical etching did not increase or decrease the Ra but modified the surface aspect by making it duller than before.

Total roughness measurements conclusions are the same as Ra for the first chemical etching (decrease of only 6.5%) and for robotic milling (decrease of 95%). Though, the last chemical etching increased Rt substantially (by 83%). These measurements have been only made on two parts. So, it would be interesting to pursue analysis and make a chemical etching with more parts robotically milled beforehand to assess this influence of chemical etching on robotic milling in terms of Rt.

Diameter measurements showed the expected results and a global decrease of part size along the experimental steps. The average material removed on each cylinder of diameter b is 1.453 mm after all different steps.

Even if the parts were coming from the same region of the building plate, cylindricity of raw parts were heterogeneous (σ = 0.027 mm for an average cylindricity of 0.062 mm). The first chemical etching did not change these results. However, robotic milling degraded cylindricity of the part by 300% due to the process itself. Chemical etching does not degrade cylindricity while robotic milling does.

Finally, this study shows the potential of chemical etching but also its limitations. This process is very promising since it allows to treat the part regardless of its geometry and without inducing stresses on the part surface. However, it was not possible to reach an arithmetic roughness as good as after robotic milling. Moreover, after having applied a chemical etching on the core material of the part, Rt increased and the shiny surface became dull. More analysis will be required to assess if this aspect modification is linked to a metallurgical change of the part surface material. These observations show that it is not yet possible to use directly chemical etching for raw parts coming from a 3D EBM machine without further analysis.

8. Acknowledgements

The author is grateful to Mr. Jonathan DUQUESNOY of Chimiderouil workshop who has performed both chemical etching of this study and to Mr. Valentin DAMBLY from the Theoretical Mechanics Department (Faculty of Engineering the University of Mons) who has performed the robotic milling of the parts. Finally, the author thanks all the colleagues and technical supervisors who helped making this study.

9. References

[1] Bourell DL. Perspectives on Additive Manufacturing. Annu Rev Mater Res. 2016;46(1):1–18.
[2] Dolimont A. PhD Thesis – Functionalization of Electron Beam Melting parts in order to guide finishing operations. University of Mons; 2018.
[3] Thompson MK, Moroni G, Vaneker T, Fadel G, Campbell RI, Gibson I, Bernard A, Schulz J, Graf P, Ahuja B, Martina F. Design for Additive Manufacturing: Trends, opportunities, considerations, and constraints. CIRP Ann - Manuf Technol. 2016;65(2):737–60.
[4] de Formanoir C, Suard M, Dendievel R, Martin G, Godet S. Improving the mechanical efficiency of electron beam melted titanium lattice structures by chemical etching. Addit Manuf [Internet]. 2016;11:71–6.
[5] Liu S, Shin YC. Additive manufacturing of Ti6Al4V alloy: A review. Mater Des. 2019;164:107552.
[6] Neikov OD. Powders for Additive Manufacturing Processing. 2nd ed. Handbook of Non-Ferrous Metal Powders. Elsevier Ltd.; 2019. 373–399 p.
[7] Bourell D, Kruth JP, Leu M, Levy G, Rosen D, Beese AM, Clare A. Materials for additive manufacturing. CIRP Ann - Manuf Technol. 2017;66(2):659–81.
[8] Nutal N. Finition de surface de pièces produites par fabrication additive. 2019;33(0):1–23.
[9] Beaucamp AT, Namba Y, Charlton P, Jain S, Graziano AA. Finishing of additively manufactured titanium alloy by shape adaptive grinding (SAG). Surf Topogr Metrol Prop. 2015;3(2).
[10] Bagehorns S, Mertens T, Greitemeier D, Carton L, Schoberth A. Surface finishing of additive manufactured Ti-6Al-4V - a comparison of electrochemical and mechanical treatments. Eucass 2015. 2015;(June).
[11] Lhuissier P, de Formanoir C, Martin G, Dendievel R, Godet S. Geometrical control of lattice structures produced by EBM through

chemical etching: Investigations at the scale of individual struts. Mater Des. 2016;110:485–93.
[12] Persenot T, Martin G, Dendievel R, Buffiére JY, Maire E. Enhancing the tensile properties of EBM as-built thin parts: Effect of HIP and chemical etching. Mater Charact. 2018;143(November 2017):82–93.
[13] Lyczkowska E, Szymczyk P, Dybała B, Chlebus E. Chemical polishing of scaffolds made of Ti-6Al-7Nb alloy by additive manufacturing. Arch Civ Mech Eng. 2014;14(4):586–94.
[14] Wysocki B, Idaszek J, Buhagiar J, Szlązak K, Brynk T, Kurzydłowski KJ, Święszkowski W. The influence of chemical polishing of titanium scaffolds on their mechanical strength and in-vitro cell response. Mater Sci Eng C [Internet]. 2019;95(2017):428–39.
[15] Dolimont A, Rivière-Lorphèvre E, Ducobu F, Backaert S. Impact of chemical polishing on surface roughness and dimensional quality of electron beam melting process (EBM) parts. In: AIP Conference Proceedings. American Institute of Physics Articles; 2018. p. 2–8.
[16] Dolimont A, Demarbaix A, Ducobu F, Rivière-Lorphèvre E. Chemical etching as a finishing process for electron beam melting (EBM) parts. AIP Conf Proc. 2019;2113:1–6.
[17] International Organization for Standardization. Geometrical Product Specifications (GPS) - Surface texture: Profile method – Rules and procedures for the assessment of surface texture. NF EN ISO 4288. 1998;